

PHOTOPRODUCTION OF Θ^+ ON THE NUCLEON AND DEUTERON

T. MART

Departemen Fisika, FMIPA, Universitas Indonesia, Depok 16424, Indonesia

A. SALAM AND K. MIYAGAWA

Department of Applied Physics, Okayama University of Science, 1-1 Ridai-cho, Okayama 700, Japan

C. BENNHOLD

Center for Nuclear Studies, Department of Physics, The George Washington University, Washington, D.C. 20052, USA

Photoproduction of the pentaquark particle Θ^+ on the nucleon has been studied by using an isobar and a Regge model. Using the isobar model, total cross sections around 100 nb for the $\gamma n \rightarrow K^- \Theta^+$ channel and 400 nb for the $\gamma p \rightarrow \bar{K}^0 \Theta^+$ process are obtained. The inclusion of the K^* intermediate state yields a substantially large effect, especially in the $\gamma p \rightarrow \bar{K}^0 \Theta^+$ process. The Regge approach predicts smaller cross sections, i.e., less than 100 nb (20 nb) for the process on the neutron (proton). By using an elementary operator from the isobar model, cross sections for the process on a deuteron are predicted.

1. Introduction

The observation of the pentaquark Θ^+ baryon¹ has triggered a great number of investigations on the production process of this unconventional particle. In general, these efforts can be divided into two categories, i.e., investigations using hadronic and electromagnetic processes. The electromagnetic (photoproduction) process is, however, well known as a more "clean" process. Furthermore, photoproduction process provides an easier way to "see" the Θ^+ which contains an antiquark, since all required constituents are already present in the initial state². Other processes, such as e^+e^- and $\bar{p}p$ annihilations, would produce the strangeness-antistrangeness from gluons, which has a consequence of the suppressed cross section³.

Several Θ^+ photoproduction studies have been performed by using iso-

bar models with Born approximation⁴, where the obtained cross section spans from several nanobarns to almost one μbarn , depending on the Θ^+ width, parity, hadronic form factor cut-off, and the exchanged particles used in the process. Those parameters are unfortunately still uncertain at present.

In this paper, we calculate the photoproduction cross sections by utilizing an isobar model. Since the production threshold is already high we compare the results with those obtained from a Regge model. The comparison is also very important, since most input parameters in the isobar model are less known.

2. Formalism

The basic background amplitudes for the processes

$$\gamma(k) + n(p) \rightarrow K^-(q) + \Theta^+(p') \quad \text{and} \quad \gamma(k) + p(p) \rightarrow \bar{K}^0(q) + \Theta^+(p')$$

are obtained from a series of tree-level Feynman diagrams shown in Fig. 1. They contain the n , Θ^+ , K^- , K^{*-} and K_1 intermediate states in the first process, whereas in the second process the \bar{K}^0 exchange does not present since a real photon cannot interact with a neutral meson. The K^* and K_1 intermediate states are considered here, since previous studies on $K\Lambda$ and $K\Sigma$ photoproductions have shown that their roles are significant.

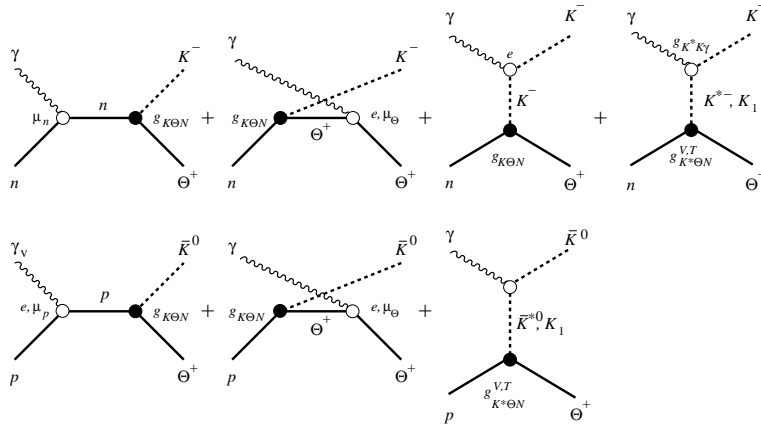


Figure 1. Feynman diagrams for Θ^+ photoproduction on neutron $\gamma + n \rightarrow K^- + \Theta^+$ (top) and on the proton $\gamma + p \rightarrow \bar{K}^0 + \Theta^+$ (bottom).

The transition matrix for both reactions can be decomposed into

$$M_{fi} = \bar{u}(\mathbf{p}') \sum_{i=1}^4 A_i M_i u(\mathbf{p}) , \quad (1)$$

where the gauge and Lorentz invariant matrices M_i are given in, e.g., Ref.¹⁷. In terms of Mandelstam variables s , u , and t , the functions A_i are given by

$$A_1 = -\frac{eg_{\Theta}}{s - m_N^2} \left(Q_N + \kappa_N \frac{m_N - m_{\Theta}}{2m_N} \right) F_1(s) - \frac{eg_{\Theta}}{u - m_{\Theta}^2 + im_{\Theta}\Gamma_{\Theta}} \times \\ \left[Q_{\Theta} + \kappa_{\Theta} \left(\frac{m_{\Theta} - m_N}{2m_{\Theta}} - i \frac{\Gamma_{\Theta}}{4m_{\Theta}} \right) \right] F_2(u) \\ - \frac{C_{K^*} G^T F_3(t)}{M(t - m_{K^*}^2 + im_{K^*}\Gamma_{K^*})(m_{\Theta} + m_N)} , \quad (2)$$

$$A_2 = \frac{2eg_{\Theta}}{t - m_K^2} \left(\frac{Q_N}{s - m_N^2} + \frac{Q_{\Theta}}{u - m_{\Theta}^2} \right) \tilde{F} + \frac{C_{K^*} G^T F_3(t)}{M(t - m_{K^*}^2 + im_{K^*}\Gamma_{K^*})} \\ \times \frac{1}{(m_{\Theta} + m_N)} - \frac{C_{K_1} G_{K_1}^T F_3(t)}{M(t - m_{K_1}^2 + im_{K_1}\Gamma_{K_1})(m_{\Theta} + m_p)} , \quad (3)$$

$$A_3 = \frac{eg_{\Theta}}{s - m_N^2} \frac{\kappa_N F_1(s)}{2m_N} - \frac{eg_{\Theta}}{u - m_{\Theta}^2} \frac{\kappa_{\Theta} F_2(u)}{2m_{\Theta}} - \frac{C_{K^*} G^T F_3(t)}{M(t - m_{K^*}^2 + im_{K^*}\Gamma_{K^*})} \\ \times \frac{m_{\Theta} - m_N}{m_{\Theta} + m_N} + \frac{(m_{\Theta} + m_p) C_{K_1} G_{K_1}^V + (m_{\Theta} - m_p) C_{K_1} G_{K_1}^T}{M(t - m_{K_1}^2 + im_{K_1}\Gamma_{K_1})(m_{\Theta} + m_p)} F_3(t) \quad (4)$$

$$A_4 = \frac{eg_{\Theta}\kappa_N}{s - m_N^2} \frac{F_1(s)}{2m_N} + \frac{eg_{\Theta}\kappa_{\Theta}}{u - m_{\Theta}^2} \frac{F_2(u)}{2m_{\Theta}} + \frac{C_{K^*} G^V F_3(t)}{M(t - m_{K^*}^2 + im_{K^*}\Gamma_{K^*})} , \quad (5)$$

with $g_{\Theta} = g_{K\Theta N}$, $Q_{\Theta} = 1$, $Q_N = 1$ (0) for proton (neutron), κ_N and κ_{Θ} indicate the anomalous magnetic moments of the nucleon and Θ^+ , and M is taken to be 1 GeV in order to make the coupling constants $G^{V,T} = g_{K^*\Theta N}^{V,T} g_{K^*K\gamma}$ dimensionless.

The inclusion of hadronic form factors at hadronic vertices is performed by utilizing the Haberzettl prescription¹⁸. The form factors are taken as

$$F_i(q^2) = \frac{\Lambda^4}{\Lambda^4 + (q^2 - m_i^2)^2} \quad \text{with} \quad q^2 = s, u, t , \quad (6)$$

with Λ the corresponding cut-off. The form factor for non-gauge-invariant terms $\tilde{F}(s, u, t)$ in Eq.(3) is extra constructed in order to satisfy crossing symmetry and to avoid a pole in the amplitude¹⁹, i.e.,

$$\tilde{F}(s, u, t) = F_1(s) + F_1(u) + F_3(t) - F_1(s)F_1(u) \\ - F_1(s)F_3(t) - F_1(u)F_3(t) + F_1(s)F_1(u)F_3(t). \quad (7)$$

Since Θ^+ is an isoscalar particle, the coupling constants relations read

$$g_{K\Theta N} = g_{K^-\Theta^+n} = g_{K^0\Theta^+p} \quad , \quad g_{K^*\Theta N}^{V,T} = g_{K^{*-}\Theta^+n}^{V,T} = g_{\bar{K}^{*0}\Theta^+p}^{V,T} . \quad (8)$$

The coupling constant $g_{K^-\Theta^+n}$ can be calculated from the decay width of the $\Theta^+ \rightarrow K^+n$ by using

$$\Gamma = \frac{g_{K^-\Theta^+n}^2}{4\pi} \frac{E_n - m_n}{m_\Theta} p , \quad (9)$$

with $p = [\{m_\Theta^2 - (m_K + m_n)^2\}\{m_\Theta^2 - (m_n - m_K)^2\}^{1/2}]/2m_\Theta$. The precise measurement of the decay width is still lacking due to the experimental resolution. The reported width¹ is in the range of 6–25 MeV. Using the partial wave analysis of K^+N data Arndt *et al.*⁵ found $\Gamma \leq 1$ MeV, whereas the PDG⁶ announces $\Gamma = 0.9 \pm 0.3$ MeV. Based on this information we use a width of 1 MeV in our calculation. Explicitly, we use

$$g_{K\Theta N}/\sqrt{4\pi} = 0.39 . \quad (10)$$

The magnetic moment of Θ^+ is also not well known. A recent chiral soliton calculation⁹ yields a value of $\mu_\Theta = 0.82 \mu_N$, from which we obtain $\kappa_\Theta = 0.35$. Note that in the second channel the Regge model does not depend on this coupling constant as well as the Θ^+ magnetic moment.

The coefficient C_{K^*} in Eqs. (2)-(5) is introduced since in \bar{K}^0 photoproduction the vector meson exchange in the t -channel is K^{*0} . The coefficient reads¹⁰

$$C_{K^*} = 1 \quad \text{for } K^-\Theta^+ \quad [-1.53 \quad \text{for } \bar{K}^0\Theta^+] . \quad (11)$$

The coupling constants $g_{K^*\Theta N}^V$ and $g_{K^*\Theta N}^T$ are also not well known. Therefore, we follow Refs. ^{4,11}, i.e., using $g_{K^*\Theta N}^V = 1.32$ and neglecting $g_{K^*\Theta N}^T$ due to the lack of information on this coupling. By combining the electromagnetic and hadronic coupling constants we obtain

$$G_{K^*\Theta N}^V/4\pi = 8.72 \times 10^{-2} . \quad (12)$$

Most previous calculations excluded the K_1 exchange, mainly due to the lack of information on the corresponding coupling constants. Reference⁴ used the vector dominance relation $g_{K_1 K \gamma} = eg_{K_1 K \rho}/f_\rho$ to determine the electromagnetic coupling $g_{K_1 K \gamma}$, where $f_\rho^2/4\pi = 2.9$ and $g_{K_1 K \rho} = 12$ is taken from the effective Lagrangian calculation of Ref. ¹⁴. As in the case of K^* , the K_1 hadronic tensor coupling will be neglected in this calculation due to the same reason. Following Ref. ⁴, the K_1 axial vector coupling $g_{K_1 \Theta N}^V$ is estimated from an isobar model for $K^+\Lambda$ photoproduction¹⁵ by using the extracted ratio $G_{K^*\Lambda N}^V/G_{K_1 \Lambda N}^V = -8.26$. We note that the same

ratio is also obtained in Ref.¹² for the model without missing resonance $D_{13}(1895)$. Therefore, in our calculation we use

$$G_{K_1\Theta N}^V/4\pi = -7.64 \times 10^{-3} . \quad (13)$$

The constant C_{K_1} in Eqs.(3) and (4) is extracted from fitting an isobar model to the $K^+\Sigma^0$ and $K^0\Sigma^+$ photoproduction data¹³, i.e.,

$$C_{K_1} = 1 \text{ for } K^-\Theta^+ \text{ } [-0.17 \text{ for } \bar{K}^0\Theta^+] . \quad (14)$$

3. Regge Model

In Regge model one should only use the K^- and K^* (K^* and K_1) diagrams in Fig.1 for the $\gamma n \rightarrow K^-\Theta^+$ ($\gamma p \rightarrow \bar{K}^0\Theta^+$) channel. Hence, the result from Regge model will not depend on the value of $g_{K\Theta N}$ and Θ^+ magnetic moment in the second channel. The procedure is adopted from Ref.¹⁶, i.e., by replacing the Feynman propagator with the Regge propagator

$$P_{\text{Regge}} = \frac{s^{\alpha_{K^i}(t)-1}}{\sin[\pi\alpha_{K^i}(t)]} e^{-i\pi\alpha_{K^i}(t)} \frac{\pi\alpha'_{K^i}}{\Gamma[\pi\alpha_{K^i}(t)]} , \quad (15)$$

where K^i refers to K^* and K_1 , and $\alpha_{K^i}(t) = \alpha_0 + \alpha' t$ denotes the corresponding trajectory¹⁶.

4. Results and Discussion

The differential cross sections obtained from the isobar model in both channels are shown in Fig. 2. Obviously, both channels show a forward peaking differential cross section which is due to the strong contribution from the K^* intermediate state. Previous studies which use only Born terms⁴ obtained

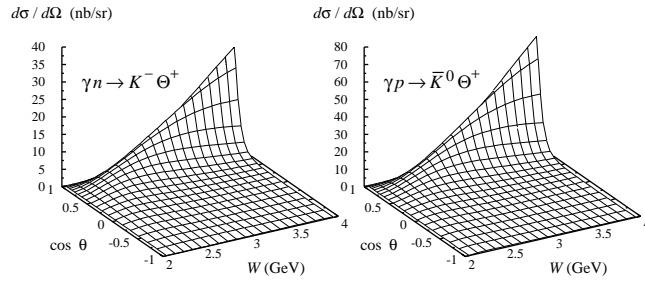


Figure 2. Differential cross sections obtained by using the isobar model.

a backward peaking cross section for the $\gamma p \rightarrow \bar{K}^0 \Theta^+$ channel, since in this case no t -channel intermediate state is included. Figure 2 also demonstrates that the hadronic form factors are unable to suppress the cross sections at higher energies.

The strong contribution of the K^* in both channels can be observed in Fig. 3, where we can see that the inclusion of this state increases the total cross sections by more than one order of magnitude. In contrast to the K^* , contribution from the K_1 vector meson is negligible. This fact can be traced back to the coupling constants given by Eqs. (13) and (14).

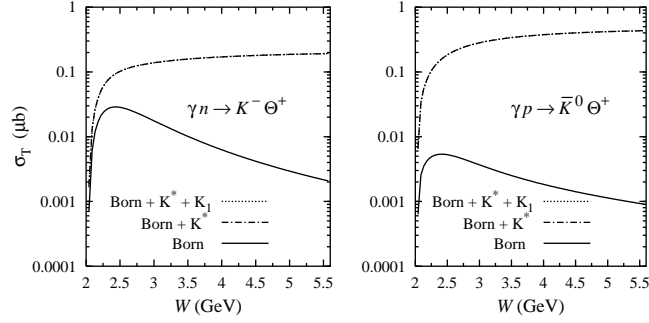


Figure 3. Contribution of the Born terms, K^* - and K_1 -exchange to the total cross sections.

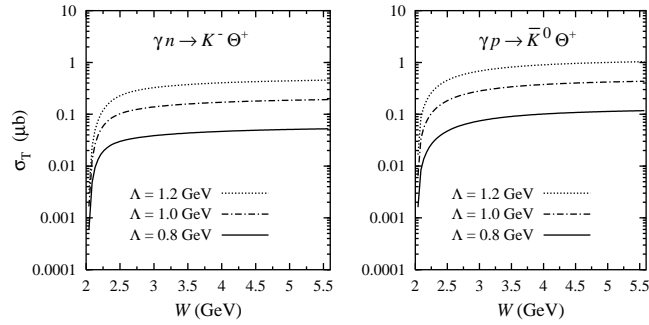


Figure 4. Total cross sections for Θ^+ photoproduction off a neutron (left) and a proton (right) as a function of the hadronic form factor cut-off Λ .

Figure 4 demonstrates the sensitivity of the total cross sections to the

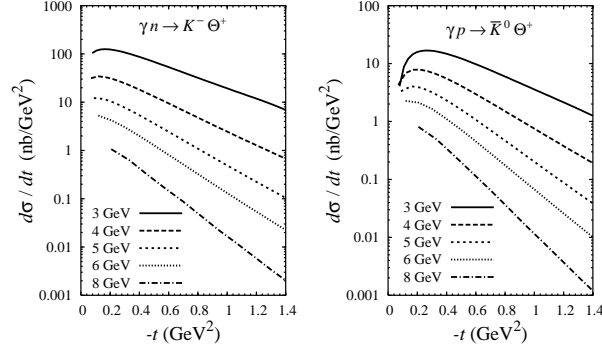


Figure 5. Differential cross section for Θ^+ photoproduction obtained from the Regge calculation. The corresponding total c.m. energy W is shown in each panel.

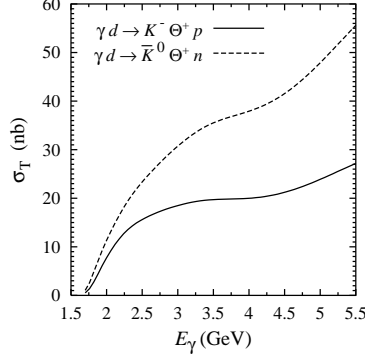


Figure 6. Total cross section for the inclusive Θ^+ photoproduction on the deuteron.

choice of the hadronic form factor cut-off. Clearly, a right choice of the cut-off is very important in this case. For this purpose, we calculate also the cross sections by using a Regge model. The results are shown in Fig. 5. Obviously, the Regge approach predicts smaller cross sections than those obtained from the isobar model. In the case of $K\Lambda$ and $K\Sigma$ photoproductions, Ref.²⁰ showed that Regge model works nicely at higher energies (up to $W = 5$ GeV) but overpredicts the $K^+\Lambda$ (underpredicts the $K^+\Sigma^0$) data at the resonance region ($W \leq 2$ GeV) by up to 50%. Thus, we would expect the same result for Θ^+ photoproduction. By comparing with the result obtained from the isobar model, we can conclude that the isobar prediction could overestimate the realistic cross section, especially at higher

energies, unless a softer hadronic form factor is chosen. This result can partly explain why the high energy experiments are unable to observe the existence of the Θ^+ .

Using the elementary operator of the isobar model we predict the inclusive total cross section for Θ^+ photoproduction on the deuteron. The results for both possible channels are given in Fig. 6, where we show the inclusive total cross section obtained by using an isobar model with $\Lambda = 0.8$ GeV. The fact that the $K^-\Theta^+$ cross section is smaller than the $K^0\Theta^+$ one is originated from the elementary process (see Fig. 3).

In conclusion, we have calculated cross sections of Θ^+ photoproduction by using an isobar and a Regge models. The Regge model predicts smaller cross sections, especially at higher energies.

The work of TM has been partly supported by the QUE project.

References

1. T. Nakano *et al.*, Phys. Rev. Lett. **91**, 012002 (2003); J. Barth *et al.*, Phys. Lett. B **572**, 127 (2003); S. Stepanyan *et al.*, Phys. Rev. Lett. **91**, 252001 (2003); V. Kubarovsky *et al.*, Phys. Rev. Lett. **92**, 032001 (2004); V.V. Barmin *et al.*, Phys. Atom Nucl. **66**, 1715 (2003); A. Airapetian *et al.*, Phys. Lett. B **585**, 213 (2004); A. Aleev *et al.*, hep-ex/0401024; S. Nussinov, hep-ph/0307357 (2003).
2. M. Karliner and H.J. Lipkin, Phys. Lett. B **597**, 309 (2004)
3. A.I. Titov, A. Hosaka, S. Date and Y. Ohashi, nucl-th/0408001.
4. B.G. Yu, T.K. Choi, and C.-R. Ji, nucl-th/0312075 and references therein.
5. R.A. Arndt, I.I. Strakovsky, and R.L. Workman, nucl-th/0311030 (2003).
6. Particle Data Group: S. Eidelman *et al.*, Phys. Lett. B **592**, 1 (2004).
7. W. Liu and C.M. Ko, nucl-th/0308034.
8. S.I. Nam, A. Hosaka, and H-Ch Kim, hep-ph/0308313.
9. Hyun-Chul Kim, hep-ph/0308242.
10. T. Mart, C. Bennhold and C.E. Hyde-Wright, Phys. Rev. C **51**, 1074 (1995).
11. W. Liu, C.M. Ko, and V. Kubarovsky, Phys. Rev. C **69**, 025202 (2004).
12. T. Mart and C. Bennhold, Phys. Rev. C **61**, 012201 (2000).
13. T. Mart, Phys. Rev. C **62**, 038201 (2000).
14. K. Haglin, Phys. Rev. C **50**, 1688 (1994).
15. R.A. Williams, C.-R. Ji, and S.R. Cotanch, Phys. Rev. C **46**, 1617 (1992).
16. M. Guidal, J.M. Laget, and M. Vanderhaeghen, Nucl. Phys. **A627**, 645 (1997).
17. F.X. Lee, T. Mart, C. Bennhold and L.E. Wright, Nucl. Phys. **A695**, 237 (2001).
18. H. Haberzettl, C. Bennhold, T. Mart, and T. Feuster, Phys. Rev. C **58**, R40 (1998).
19. R.M. Davidson and R. Workman, Phys. Rev. C **63**, 025210 (2001).
20. T. Mart and T. Wijaya, Acta Phys. Polon. B **34**, 2651 (2003).